Journal of Alloys and Compounds 509 (2011) 3952–3957

Contents lists available at ScienceDirect

Journal of Alloys and Compounds

journal homepage: www.elsevier.com/locate/jallcom

Structural and hyperfine properties of $Ti_{48}Zr_7Fe_{18}$ nano-compounds and its hydrides

A. Żywczak[a], Ł. Gondek[a,*], H. Figiel[a], J. Żukrowski[a], J. Czub[a], A. Takasaki[b]

[a] Faculty of Physics and Applied Computer Science, AGH University of Science and Technology, Mickiewicza 30, 30-059 Kraków, Poland
[b] Department of Engineering Science and Mechanics, Shibaura Institute of Technology, Toyosu, Koto-ku, Tokyo 135-8548, Japan

ARTICLE INFO

Article history:
Received 20 September 2010
Accepted 28 December 2010
Available online 4 January 2011

PACS:
61.10.Nz
61.44.Br
61.43.Er
65.50.+m

Keywords:
Disordered systems
Quasicrystals
X-ray scattering
Thermodynamic properties

ABSTRACT

It is well established that Ti-based nano-alloys are able to absorb hydrogen with relatively high hydrogen to metal ratio of 4/3. In this study the $Ti_{48}Zr_7Fe_{18}$ nano-compound, prepared by mechanical alloying (MA), has been investigated. In its initial state the compound is amorphous, however upon thermal treatment it transforms to the quasicrystalline icosahedral structure (i-phase), which is based on the Mackay cluster type. Structural characterization of the sample was made by means of XRD measurements. Thermodynamic properties were studied by differential scanning calorimetry (DSC) and thermal desorption spectroscopy (TDS). To find the influence of hydrogen and structure type on hyperfine interactions the Mössbauer spectroscopy (MS) experiment was performed, as well. The amorphous sample after MA was hydrogenated in order to unveil hydrogen influence on crystal properties of the sample. Upon hydrogenation of the amorphous sample a decomposition into simple hydrides took place.

1. Introduction

The icosahedral (i) quasicrystal phase in Ti–Zr–Ni system was discovered by Kim and Kelton [1]. According to the literature, i-phases based on TiZrNi and TiZrFe compositions could be used as hydrogen storage materials [2–4].

The structure of $Ti_{48}Zr_7Fe_{18}$ is based on the Mackay cluster (Ti – Mackay class). It consists of two inner and outer shells of atoms possessing 55 atoms per cluster. The inner shell (icosahedron) contains 13 atoms: a Fe atom in the centre and 12 Ti atoms occupying the vertices of the icosahedron. The outer cluster consists of 42 atoms: 12 Fe atoms forming an icosahedron, 24 Ti atoms and 6 Zr atoms occupying the vertices of the faces of this icosahedron [5]. This $Ti_{48}Zr_7Fe_{18}$ cluster contains 20 tetrahedral interstitial sites in the central shell, and 60 tetrahedral and 20 octahedral interstitial sites in the outer shell. The total number of atoms in $Ti_{48}Zr_7Fe_{18}$ cluster is 73, while the maximum number of absorbed hydrogen atoms can be equal to the number of interstitial sites reaching 100. Therefore $Ti_{48}Zr_7Fe_{18}$ quasicrystal has a possibility to absorb hydrogen with the maximum H/M ratio of 100/73–1.37 [6–8].

2. Experimental

The $Ti_{48}Zr_7Fe_{18}$ samples were produced of commercially pure titanium (99.9%), zirconium (99.9%) and iron (99.9%) powders by mechanical alloying (MA) and subsequent annealing as described for $Ti_{45}Zr_{38}Ni_{17}$ reported in Ref. [9–11]. The total MA time was 40 h and for the produced powders the XRD measurements were performed to check the quality and get structural information about the products. Then, the produced powders were annealed at 715 K in a vacuum furnace (3×10^{-3} Pa) to obtain the quasicrystalline i-phase.

The structural and thermodynamic properties, and hyperfine parameters of the produced compounds and its hydrides were characterized by means of X-ray diffraction (Cu Kα), differential scanning calorimetry (DSC), thermal desorption spectroscopy (TDS) and Mössbauer spectroscopy (MS).

The chemical compositions of the produced powders were determined by means of the energy dispersive X-ray spectroscopy (EDS) using IB Zeiss Neon 40EsB CrossBeam equipped with QUANTAX EDS system. Two samples of the materials studied (amorphous and i-phase) were prepared for the investigation. The powdered samples were mixed with epoxy resin (G-1 Epoxy Kit, Gatan), placed onto a 3 mm diameter copper slot and heated for 1 h at a temperature of 150 °C.

The obtained powders were hydrogenated in a high-pressure stainless-steel vessel. The vessel was filled with pure (99.9999%) hydrogen gas and heated at a constant temperature of 573 K. The initial hydrogen pressure at 573 K was 3.8 MPa. The samples were hydrogenated for 120 h. The hydrogen concentration in the sample was determined from hydrogen pressure change in the vessel.

The standard differential scanning calorimetry (DSC) measurements were made under argon gas flow at a heating rate of 5 K/min. The hydrogen desorption kinetics was analyzed by a thermal desorption spectrometer (TDS) equipped with a quadrupole mass analyzer. The sample powder was mounted in an infrared vacuum furnace (10^{-6} Pa), and sample was heated up to 950 K at a constant heating rate. During heating, the hydrogen partial pressure (ion current of H_2) which corresponds

* Corresponding author. Tel.: +48 12 6172904.
E-mail address: lgondek@agh.edu.pl (Ł. Gondek).

0925-8388/$ – see front matter © 2011 Elsevier B.V. All rights reserved.
doi:10.1016/j.jallcom.2010.12.186

Table 1
The chemical compositions (wt%) of the amorphous and the quasicrystalline $Ti_{48}Zr_7Fe_{18}$ samples.

	Ti [wt%]	Fe [wt%]	Zr [wt%]	Error [wt%]
$Ti_{48}Zr_7Fe_{18}$ amorphous	60.0	24.7	15.3	3
$Ti_{48}Zr_7Fe_{18}$ i-phase	60.5	24.7	14.8	3
Formal composition	58.3	25.5	16.2	–

directly to the rate of hydrogen desorption, was monitored by the quadrupole mass analyzer [9–11].

The ^{57}Fe Mössbauer spectroscopy (MS) measurements were carried out in the 4.2–300 K temperature range by means of a standard MS spectrometer. The set up was operated in sine-mode using ^{57}Co(Rh) source operating in the room temperature. The α-Fe foil was used as a calibration standard. The powder samples were encapsulated in a high purity Al foil. The obtained spectra were analysed in terms of the standard least-squares fitting procedure.

3. Results and discussion

3.1. Structural characterization

The EDS analyses of amorphous and i-phase samples were performed to confirm its chemical composition and homogeneity. The studies were made at several different points of the samples. The investigations revealed that the concentrations of the particular elements at each point are identical within error bars. The mean values of relative element concentrations in at% are presented in Table 1.

Fig. 1(a) presents XRD pattern of $Ti_{48}Zr_7Fe_{18}$ sample obtained directly after MA. The pattern indicates that the obtained powder sample was amorphous and it was not possible to distinguish diffraction peaks related to any type of crystal structure, besides the traces of Ti_2Fe type crystal phase.

The obtained amorphous powder sample was annealed in a furnace to find whether the i-phase would appear. Fig. 1(b) presents XRD pattern for the amorphous powder sample after annealing at 715 K. The reflections in the XRD patterns are well resolved and most of them can be indexed and attributed to the quasicrystalline i-phase. The peaks for the i-phase were indexed using the scheme reported by Bancel et al. [12]. Apart from the i-phase, the other peaks were indexed as the Ti_2Fe-type crystal phase which appeared similarly as the Ti_2Ni in the i-phase $Ti_{45}Zr_{38}Ni_{17}$ compound [10]. Thus, we conclude that the amorphous phase produced during MA transformed to the i-phase mainly with a small amount of Ti_2Fe phase. Hereafter, this powder is referred to as the i-phase powder.

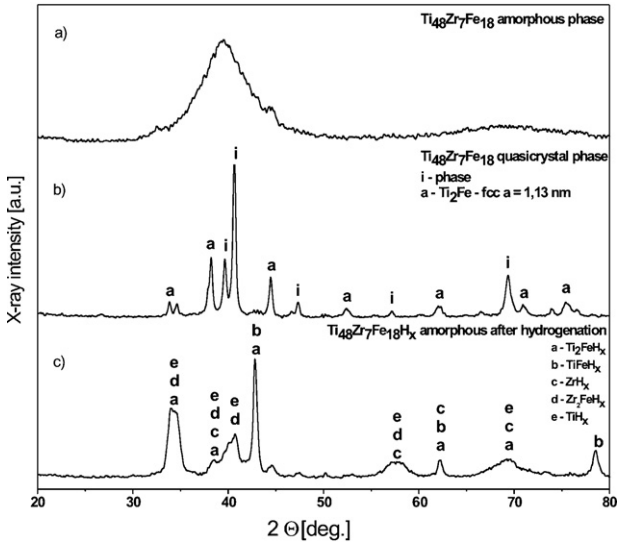

Fig. 1. X-ray diffraction patterns for the $Ti_{48}Zr_7Fe_{18}$ (a) after mechanical alloying, (b) i-phase obtained after subsequent annealing at 715 K, and (c) amorphous phase after hydriding at 573 K.

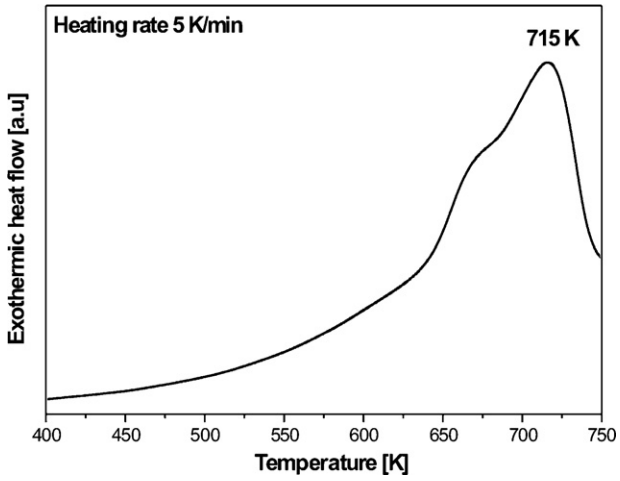

Fig. 2. DSC curve for the $Ti_{48}Zr_7Fe_{18}$ amorphous powder obtained after MA for 40 h.

Fig. 1(c) presents XRD pattern for amorphous $Ti_{48}Zr_7Fe_{18}$ phase after hydrogenation at 573 K. When one compares this pattern with XRD patterns of the starting amorphous and the i-phase powders, one can observe the effect of crystallization with appearance of many new peaks which are not directly related to the i-phase. This result suggests that upon hydriding the amorphous phase underwent decomposition into several other phases. It was possible, using Rietveld fitting procedure, to index the observed XRD peaks to TiH_2, ZrH_x, Zr_2FeH_x, $TiFeH_x$ and Ti_2FeH_x phases as labeled in Fig. 1c. The reason of such a decomposition of amorphous phase to the simple hydrides instead of amorphous hydride is probably due to energetically more efficient way for simple hydrides formation than remaining as amorphous hydride.

3.2. Calorimetric and thermal stability studies

To find the temperature of transformation from amorphous to i-phase the DSC measurements were performed Fig. 2 shows DSC curve for the amorphous $Ti_{48}Zr_7Fe_{18}$ powder, at the temperature range between 500 K and 750 K. Existence of a peak at ~715 K is due to the i-phase formation. The observed behaviour is analogous to that of the $Ti_{45}Zr_{38}Ni_{17}$system as reported in Ref. [10].

The hydriding of the amorphous sample, performed at 573 K at pressure of 3.8 MPa, was well below the temperature of the i-phase formation. The obtained hydrogen concentration correspond to 1.1 H/M (hydrogen to metal ratio), which is less than the theoretical value of 1.37 [6], or 2.01 wt% for the i-phase

To check the formation of the simple hydrides ($TiFeH_x$, Zr_2FeH_x, Ti_2FeH_x, TiH_2 and ZrH_2) as supposed in the analysis of XRD pattern for $Ti_{48}Zr_7Fe_{18}H_x$, we performed TDS experiment, because their decomposition peaks should be visible in the TDS experiment. Fig. 3 shows TDS spectrum for the $Ti_{48}Zr_7Fe_{18}H_x$ sample with three main peaks, namely a significant peak at 620 K, a broad and the strongest peak at 750 K and a small peak at 850 K. Labeled with a, b and c correspond to the decomposition temperatures of the simple hydrides $TiFeH_x$, Zr_2FeH_x, Ti_2FeH_x, TiH_x and ZrH_x, corresponding to simple hydride as observed in the analysis of the XRD pattern (Fig. 1c). It is worth noting here that the relative high intensities of XRD lines for Zr_2FeH_x and ZrH_x well correspond to the strongest peak in the TDS curve which means that they are the major products of hydriding.

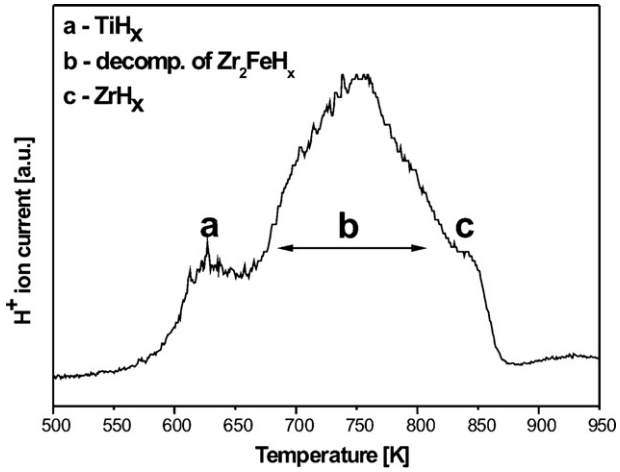

Fig. 3. TDS spectrum for the $Ti_{48}Zr_7Fe_{18}$ amorphous powder obtained after MA for 40 h.

The first peak in TDS spectrum (Fig. 3) comes from decomposing of TiH_x, which desorption temperature is 643 K. TiH_x originates from decomposition of $TiFeH_x$ into TiH_x + Fe at about 493 K [13]. The Zr_2FeH_x decomposes in between 600 and 900 K into simple phases and hydrides with releasing hydrogen, as well [14]. From those products the ZrH_x is well pronounced in our experimental curve at about 850 K.

3.3. Mössbauer spectroscopy

The MS probes the local environment of the given Mössbauer nuclei. Such measurements may be useful for analysing local atomic structures as well as magnetic properties of the studied samples. In the first case a different local topology raises some distribution of the isomeric shift (δ) and the quadrupolar splitting (QS). In the latter case, the nuclei may be exposed to a magnetic effective field originating from hyperfine interactions due to ordered magnetic moments in the sample.

The measurements performed for the amorphous sample at 300, 80 and 4.2 K, shown in Fig. 4, revealed a complex nature of the spectra. The broadened, strongly asymmetric doublet-like feature was observed at each temperature yielding some distribution of the δ and QS. The standard approach by Rancourt and Ping [15] is often used for estimation of QS distribution with some linear dependence between QS and δ. However, this method works well with more symmetrical spectra, where distribution of QS is considered to be more important than that of δ. Strong asymmetry of the collected spectra hints a significant distribution of isomer shift, thus in our case a modified model was applied.

In frames of this modification the analysis of the data was made assuming primary importance of isomer shift distribution $P(\delta)$. The distribution of the quadrupolar splitting P(QS) followed the linear relation to the $P(\delta)$. The isomer shift was defined as a position of the Lorenzian doublet centre as related to the zero velocity, whereas the QS were defined as a separation between elementary lines of the Lorenzian doublet.

In Figs. 5 and 6 the results of analysis performed are presented, where the distributions are relatively broad. At 300 K the mean δ is close to −0.25 mm/s, and its distribution seems to be relatively narrow when compared to $P(\delta)$ corresponding to the δ distributions obtained at lower temperatures. The relevant mean QS (Fig. 6) reached nearly 0.22 mm/s. At 80 K the $P(\delta)$ exhibits more broad distribution of δ with centre at −0.27 mm/s and corresponding QS is equal to 0.24 mm/s. When lowering temperature down to 4 K some further broadening of the spectrum took place. It is clearly

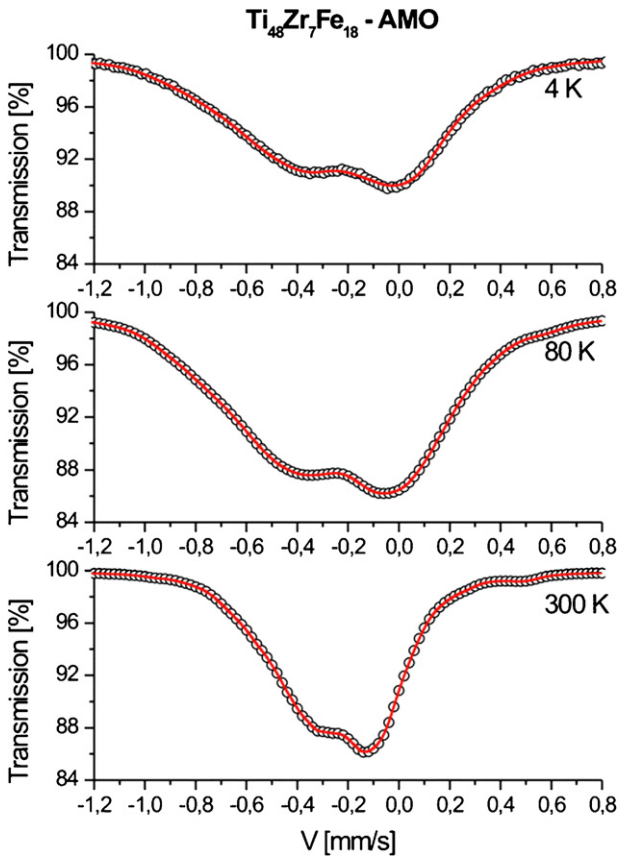

Fig. 4. The Mössbauer spectroscopy data for amorphous $Ti_{48}Zr_7Fe_{18}$ with the fit based on the modified model as described in the text.

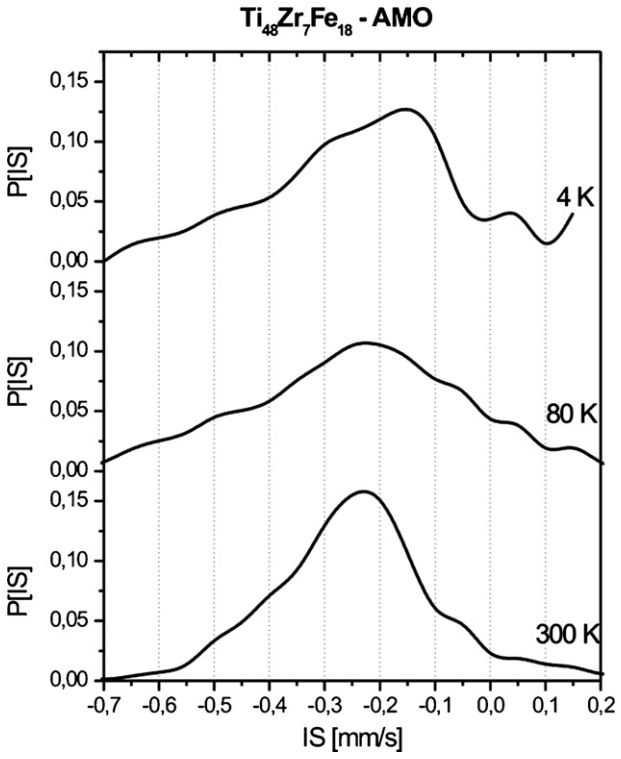

Fig. 5. Distribution of the isomeric shift for the amorphous $Ti_{48}Zr_7Fe_{18}$ sample.

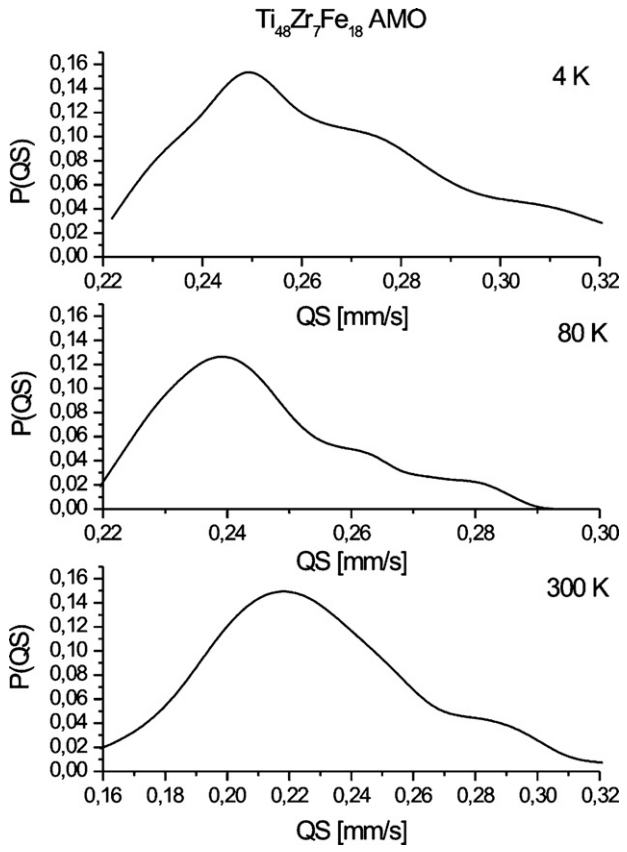

Fig. 6. Quadrupole splitting distributions for the amorphous $Ti_{48}Zr_7Fe_{18}$ sample.

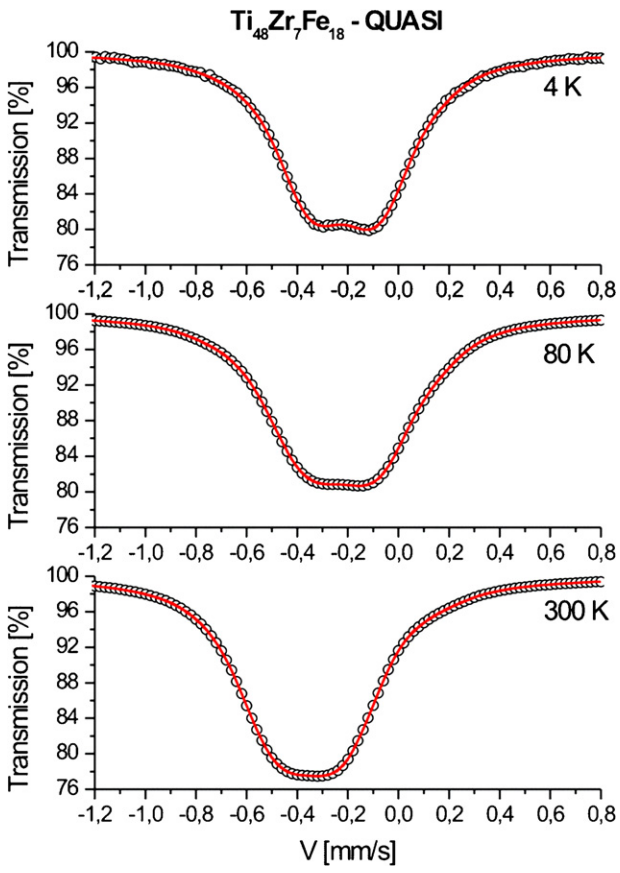

Fig. 7. Mössbauer spectroscopy data for quasicrystal sample fitted with the model as described in the text.

noticeable as an increase of the mean value of QS up to 0.26 mm/s. The mean isomeric shift became little lower with respect to higher temperatures.

The fitted spectra as collected for the quasicrystal sample of $Ti_{48}Zr_7Fe_{18}$ are shown in Fig. 7, and the distribution functions of δ and QS ate presented in Figs. 8 and 9 respectively. Within the studied temperature range, the $P(\delta)$ exhibits a bimodal behaviour. The mean δ at 300 K is close to −0.37 mm/s and became smaller at lower temperatures. Similarly to amorphous sample, the broadening of the spectra with decreasing of the temperature can be noticed, however it is not so spectacular. The bimodal character might be related to a structural characteristic of the icosahedral quasicrystal. Namely, existence of two positions of Fe with different ligand distribution is likely to be the origin of such behaviour. The QS distribution is fairly narrow with mean values between 0.20 and 0.28 mm/s.

The Mössbauer spectra recorded for hydrided amorphous sample (Fig. 10) are substantially different from those discussed above amorphous and quasicrystal samples. At first, the isomer shift distribution (Fig. 11) is much narrower than that for amorphous sample and there are no distinct doublet-like features. Secondly, the numerical analysis brought distribution of $P(\delta)$ with extremely small QS values (the spectra were deconvoluted nearly into singlet-like lines). All those, corroborate a decomposition of the amorphous sample into some simple hydrides, where the applied model is not relevant. The obtained spectra correspond well with the assumption of the overlap of the spectra coming from simple hydrides $TiFeH_x$, Ti_2FeH_x and Zr_2FeH_x. The values of isomer shift for investigation powder were in good agreement with the those reported for related alloys such as TiFe – 0.145 mm/s [16], Ti_2Fe is – 0.25 mm/s with QS in this compounds is 0.20 [17], and Zr_2FeH_x is – 0.31 mm/s with QS in this sample is 0.75.

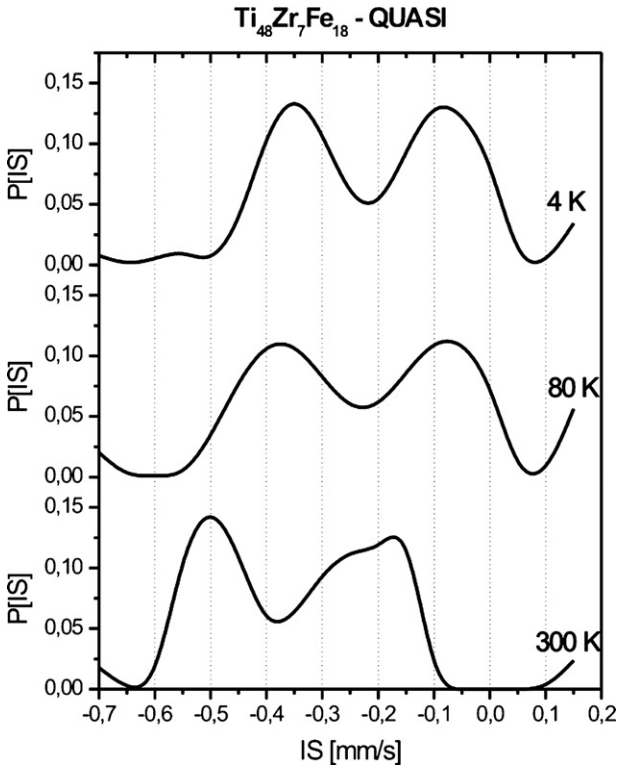

Fig. 8. Distribution of the isomeric shift for the quasicrystal sample.

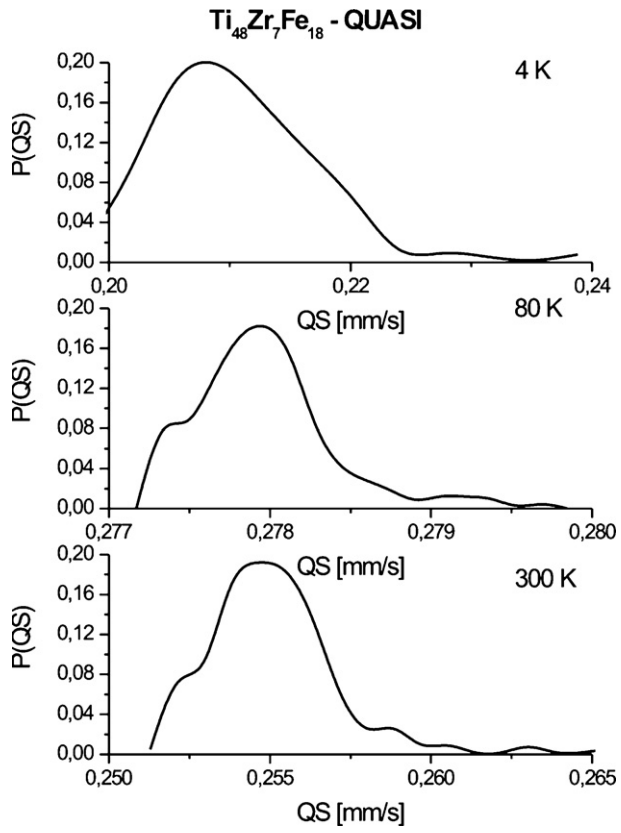

Fig. 9. Quadrupole splitting distribution for the quasicrystal $Ti_{48}Zr_7Fe_{18}$ sample.

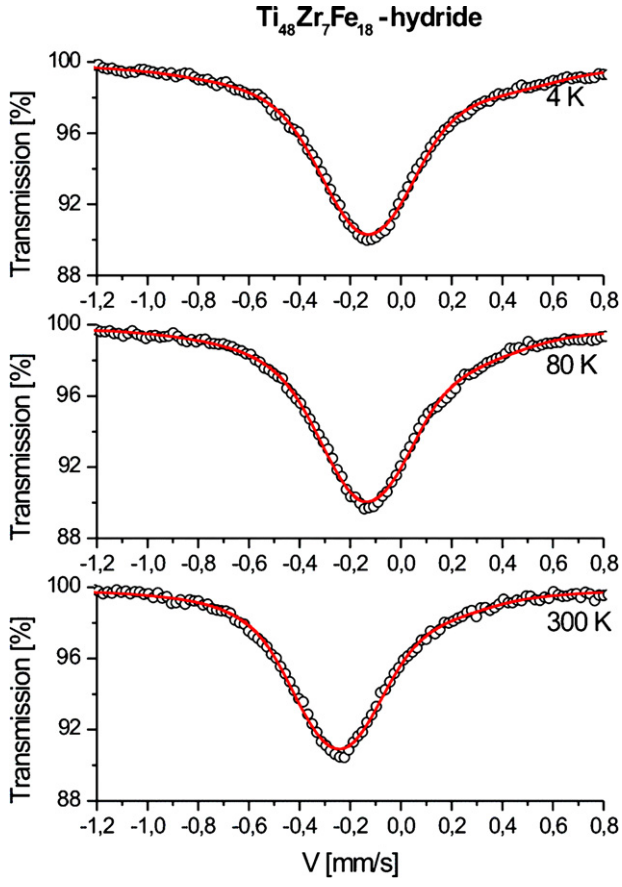

Fig. 10. Mössbauer spectroscopy data for hydrided amorphous sample ($Ti_{48}Zr_7Fe_{18}H_x$) fitted with a model as described in the text.

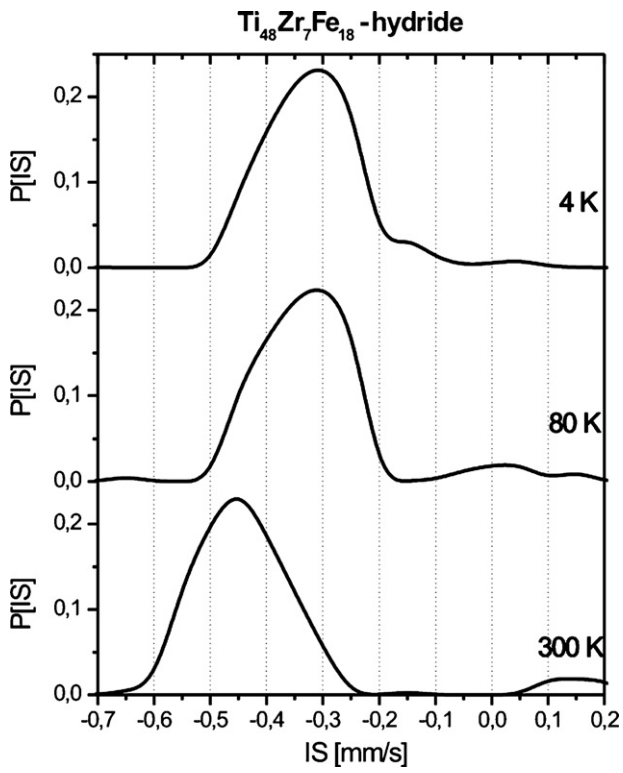

Fig. 11. Distribution of the isomeric shift for the hydrogenated $Ti_{48}Zr_7Fe_{18}H_2$ sample.

4. Conclusions

The amorphous $Ti_{48}Zr_7Fe_{18}$ powder produced during MA transformed to the i-phase with a small amount of Ti_2Fe phase after annealing.

During hydriding the amorphous powder converted into simple metal hydrides ($TiFeH_x$, Zr_2FeH_x, Ti_2FeH_x, TiH_2 and ZrH_2).

The values of isomer shift observed for investigated powder were in good agreement with the those reported for above mentioned hydrides.

Observed changes of QS and IS distributions caused by hydrogenation of the samples also proved the hydrogen driven decomposition of the compound. For the investigated $Ti_{48}Zr_7Fe_{18}$ samples (amorphous, i-phase and hydride) the lack of sextet-like features relevant to magnetic hyperfine interactions hints that there was no trace of magnetic ordering down to 4.2 K.

Acknowledgements

A part of this study was supported by the European Commission (project Dev–BIOSOFC, FP6-042436, MTKD–CT-2006-042436). The authors would like to thank MSc A. Gruszczyński (AGH-UST) for EDS and SEM investigations.

References

[1] W.J. Kim, K.F. Kelton, Philos. Mag. A 72 (1995) 1397.
[2] W.J. Kim, K.F. Kelton, Philos. Mag. Lett. 74 (1996) 439.
[3] A.M. Viano, R.M. Stroud, P.C. Gibbons, A.F. McDowell, M.S. Conradi, K.F. Kelton, Phys. Rev. B 51 (1995) 12026.
[4] P.C. Gibbons, K.F. Kelton, in: Z.M. Stadnik (Ed.), Physical Properties of Quasicrystals, Springer, Berlin, 1999, p. 403.
[5] W.J. Kim, P.C. Gibbons, K.F. Kelton, W.B. Yelon, Phys. Rev. B 58 (1998) 2578.
[6] K.F. Kelton, P.C. Gibbons, MRS Bull. 22 (1997) 69.
[7] K.F. Kelton, A.M. Viano, R.M. Stroud, E.H. Majzoub, P.C. Gibbons, S.T. Misture, in: A.I. Goldman, M.J Kramer, A.I. Goldman, D.J. Sordelet, P.A. Thiel, J.M. Dubois

(Eds.), New Horizon in Quasicrystals, Research and Applications, World Scientific, Singapore, 1997, p. 272.
[8] K.F. Kelton, J.Y. Kim, E.H. Majzoub, P.C. Gibbons, A.M. Viano, R.M. Stroud, in: S. Takeuchi, T. Fujiwara (Eds.), Proc. Sixth Intl. Conf. on Quasicrystals, World Scientific, Singapore, 1997, p. 261.
[9] A. Takasaki, C.H. Han, Y. Furuya, K.F. Kelton, Philos. Mag. Lett. 82 (2002) 353–361.
[10] A. Takasaki, K.F. Kelton, J. Alloy Compd. 347 (2002) 295.
[11] A. Żywczak, D. Shinya, Ł. Gondek, A. Takasaki, H. Figiel, Solid State Commun. 150 (2010) 1–4.
[12] P.A. Bancel, P.A. Meiney, P.W. Stephens, A.I. Goldman, P.M. Horn, Phys. Rev. Lett. 54 (1985) 2422.
[13] C.H. Chiang, Z.H. Chin, T.P. Perng, J. Alloy Compd. 307 (2000) 259–265.
[14] M. Hara, R. Hayakawa, Y. Kaneko, K. Watanabe, J. Alloy Compd. 352 (2003) 218–225.
[15] D.G. Rancourt, J.Y. Ping, Nucl. Instrum. Methods Phys. Res. B 58 (1991) 85.
[16] E. Mielczarek, W. Winfree, Phys. Rev. B 11 (1975) 1026.
[17] Y. Nakamura, K. Sumiyama, H. Ezawa, Hyperfine Interact. 27 (1986) 361–364.